Efficient heat integration of industrial CO2 capture and district heating supply

Citation for the original published paper (version of record):
Eliasson, Å., Fahrman, E., Biermann, M. et al (2022). Efficient heat integration of industrial CO2 capture and district heating supply. International Journal of Greenhouse Gas Control, 118.
http://dx.doi.org/10.1016/j.ijggc.2022.103689

International Journal of Greenhouse Gas Control 118 (2022) 103689

Contents lists available at ScienceDirect

International Journal of Greenhouse Gas Control

journal homepage: www.elsevier.com/locate/ijggc

Efficient heat integration of industrial CO_2 capture and district heating supply

Åsa Eliasson, Elin Fahrman, Maximilian Biermann, Fredrik Normann [*], Simon Harvey

Department of Space, Earth and Environment, Division of Energy Technology, Chalmers University of Technology, Gothenburg S41298, Sweden

ARTICLE INFO

Keywords:
Carbon capture
District heating
Excess heat
Specific cost
Seasonal variations
Process industry

ABSTRACT

Excess heat from industrial processes can be used for carbon capture and storage (CCS) as well as providing heat to a district heating network, leading to increased energy efficiency and reduction of on-site and/or off-site CO_2 emissions. In this work, both options are assessed with respect to economic performance and potential reduction of CO_2 emissions. The work includes a generic study based on five heat load curves for each of which three CO_2 capture plant configurations were evaluated. The economic assessment indicates that the specific cost of capture ranges from 47-134 €/t CO_2 depending on heat profile and capture plant configuration. Having excess heat available during a long period of the year, or having a high peak amount of heat, were shown to lead to low specific capture costs. The paper also includes results of a case study in which the methodology was applied to actual seasonal variations of excess heat for an integrated steel mill located in northern Sweden. Specific capture costs were estimated to 27-44 €/t CO_2, and a 36% reduction of direct plant emissions can be achieved if the CO_2 capture plant is prioritized for usage of the available excess heat.

1. Introduction

The industry sector accounts for a significant fraction of global CO_2 emissions. One measure to reduce CO_2 emissions is to recover available residual heat, often denoted "excess heat". Excess heat may be used internally in the process to decrease primary energy usage, or externally, for e.g. district heating, thereby decreasing energy usage elsewhere. In Sweden, the expansion of district heating networks over the past decades has led to substantially decreased CO_2 emissions from the heating sector (Werner, 2017). Part of this reduction stems from the utilization of industrial excess heat, since the emissions related to such heat have typically been allocated to the main products of the industrial plant, thereby the use of industrial excess heat for district heating is normally considered to be emissions-free – although there are extensive ongoing discussions about whether industrial excess should be categorised as CO_2-free or CO_2-neutral, as summarized in a recent paper by Pelda et al. (2020). As a result, many studies have pointed out that further expansion of district heating networks would be a cost-effective option to reduce emissions in the EU energy system (e.g. Connolly et al., 2014; Manz et al., 2021). Möller et al. (2019) estimate that up to 71% of the urban heating demand can be met by district heating in 14 analyzed EU member states. Of this, up to 78% could be supplied by excess heat. However, other studies have pointed out that utilizing excess heat for district heating can have different levels of impact on the net change in emissions from the heating sector, depending on the heat supply option that is replaced, the applied system boundaries, and the assumptions about future energy market scenarios (Broberg et al., 2014; Ivner and Broberg Viklund, 2015; Olsson et al., 2015; Pettersson et al., 2020).

Carbon capture and storage (CCS) is an emerging technology that can utilize considerable amounts of industrial excess heat. CCS has been acknowledged as a technology that will be important in limiting global warming, both by enabling emissions reduction through retrofitting of existing plants in the near-term and, in the long-term, by contributing to reduction of hard-to-abate-process emissions as well as enabling negative emissions by capturing biogenic emissions (IEA, 2020; Rogelj, 2018). Although large-scale deployment of CCS has so far been slow due to lack of incentives (e.g. policy support), many new CCS projects have been announced in recent years. The reason for the new-found interest in CCS is that it is now perceived as an enabling technology to reach net-zero corporate and national emission targets, compliant with the Paris agreement (IEA, 2020). Chemical absorption using an amine solvent is widely considered to be the most mature CO_2 capture technology that is suitable for retrofitting of industrial plants. Aqueous monoethanolamine (MEA) was long considered as the benchmark solvent for amine-based capture (Oh et al., 2016). More recently,

* Corresponding author.
E-mail address: fredrik.normann@chalmers.se (F. Normann).

https://doi.org/10.1016/j.ijggc.2022.103689
Received 7 July 2021; Received in revised form 15 February 2022; Accepted 2 May 2022
Available online 6 May 2022

Nomenclature

AMP	2 amino 2 methyl 1 propanol
BFG	blast furnace gas
CAPEX	capital expenditures
CCS	carbon capture and storage
CEPCI	chemical engineering plant cost index
CHP	combined heat and power
DH	district heating
EDF	enhanced detailed factor
EIC	equipment installed cost
IEA	international energy agency
MEA	monoethanolamine
MH	maximum amount of available excess heat
OPEX	operational expenditures
PZ	piperazine
SL	seasonal length
TDC	total direct cost
TIC	total installed cost

2-amino-2-methyl-1-propanol (AMP) promoted with piperazine (PZ) has been the subject of increased interest (Feron et al., 2020). CO_2 capture requires both high capital expenditures (CAPEX), as well as large amounts of heat for regeneration of the solvent and thus high operating expenditures (OPEX) (Garðarsdóttir et al., 2018). Previous studies have therefore focused on reducing cost to facilitate the implementation of CCS. Garðarsdóttir et al. (2018) investigated the influence of flowrate and concentration of the CO_2 source on CAPEX for CO_2 capture. They concluded that both parameters have a high influence on the specific investment cost (cost per unit amount of captured CO_2), with increased flowrate or CO_2 concentration of the emission source resulting in a decrease in specific CAPEX. On the other hand, Biermann et al. (2018) found that depending on site conditions, the specific cost of capture may be decreased if partial capture (capturing <90% of the CO_2) is applied instead of full capture (defined as capturing 90% of the CO_2 from the source), despite the disadvantage of smaller scale, due to reduced specific heat supply cost and decreased heat demand. Recovery of available excess heat from the industrial plant to drive the CCS capture unit is clearly an attractive option for increasing energy efficiency and reducing the specific cost, hence making the operation of a CO_2 capture plant more economically feasible (Andersson et al., 2016; Biermann et al., 2019; Biermann et al., 2021; Sundqvist et al., 2018). In a recent study by Johnsson et al. (2020), the costs required to install and operate amine-based post-combustion CO_2 capture were mapped for all 28 manufacturing plants in Sweden with annual emissions of 500 kt CO_2 or more, of both fossil and of biogenic origin, and included a petrochemical site, refineries, iron and steel plants, cement plants and pulp and paper mills. The work considered differences in the investment required as well as differences in potential for using excess heat to cover the steam demand of the capture process, and concluded that full CO_2 capture applied to the 28 industrial plants would capture emissions corresponding to 50% of Swedish total CO_2 emissions (from all sectors) at a cost ranging from around 40 €/t CO_2 to 110 €/t CO_2, depending on emission source.

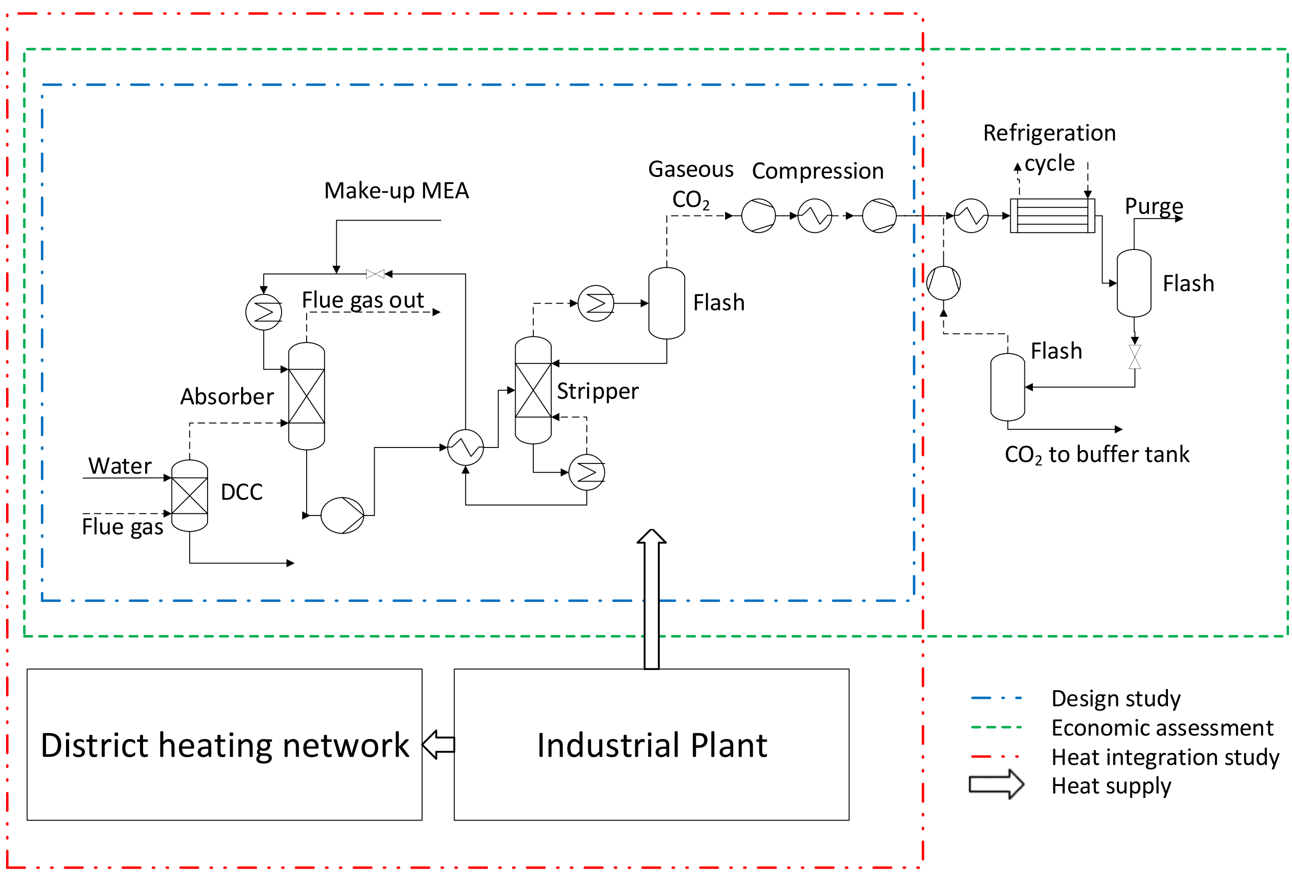

Fig. 1. An overview of the methodology and the studied system. The red border indicates the scope of the heat integration study, the blue border shows the boundaries of the design study, while the green border indicates the scope of the economic assessment. The arrows indicate heat supply from one system to another. DCC = Direct Contact Cooler; MEA = Monoethanolamine.

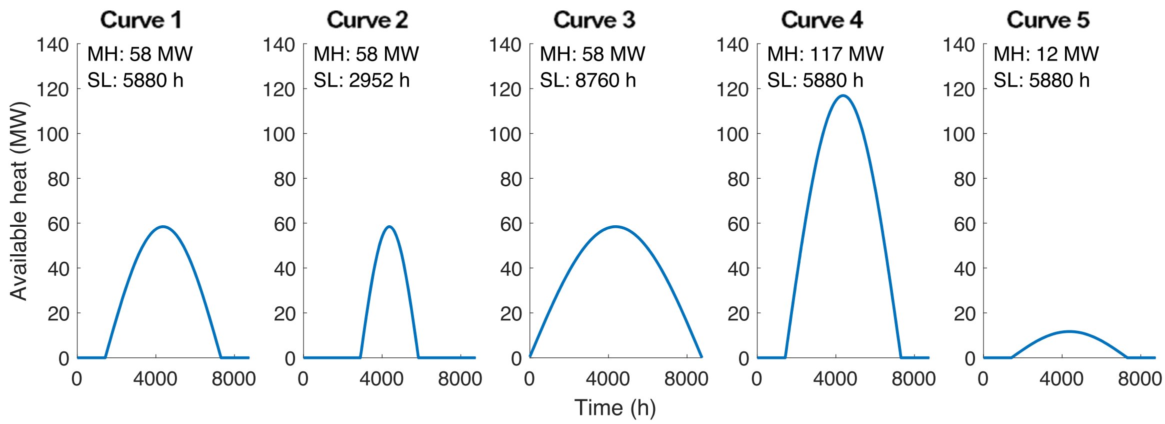

Fig. 2. Theoretical heat load curves evaluated in the generic study, defined by their seasonal length (SL, hours/year) and maximum amount of available heat (MH, MW).

Although most studies of opportunities to reduce industrial CO_2 emissions focus on single technology options, it is important to consider the effect of implementing different CO_2 mitigation options in relation to or in combination with each other. Jönsson and Algehed (2010) investigated the emissions reduction potential and economic performance of implementing district heating and CCS (among other options) at a kraft pulp mill. Eriksson et al. (2018) compared the economic feasibility of increased energy efficiency at a chemical complex site with heat recovery for external utilization. The interplay between CCS and district heating as well as the potential heat integration between them have been investigated in some studies, mostly in relation to implementation of CCS in the power generation sector. Bartela et al. (2014), for example, found that the cost of implementation of CCS at a super-critical coal--fired combined heat and power (CHP) plant could be significantly reduced if residual heat is recovered from the capture plant and delivered to a district heating network. Huang et al. (2017) examined the performance of a natural gas combined cycle-CHP plant configured to deliver heat to a district heating network as well as supplying heat to a CCS plant. It was assumed that the district heating supply should be prioritized, and alternative options for heat supply for CCS were investigated so as to achieve a 90% CO_2 capture rate all year round, i.e., despite the fluctuating district heating demand. It was concluded that the most technically and economically feasible option was supplementary firing in the heat recovery steam generators, which led to lower CO_2 emissions per unit product as compared to the other heat supply options, as well as relatively constant levels of CO_2 emissions per unit of product despite the fluctuating district heating supply.

This work compares the economic performance of possible strategies for using industrial excess heat for supplying heat to a CCS unit and a district heating network. The options investigated include strategies for design and operation of the CO_2 capture plant and their impact on how the excess heat is divided between the CCS unit and the district heating network. It is assumed that the industrial plant runs at constant capacity throughout the year, thus, the total amount of excess heat that can be delivered to the two heat sinks is constant. Heat pumps could be used to boost heat supply to the carbon capture unit by recovering low-grade excess heat discharged from the industrial plant, as suggested by Andersson et al. (2016). It could also be possible to recover low-grade residual heat from the carbon capture unit itself, as discussed in, e.g., Andersson (2020) and Hammar (2022). This was, however, beyond the scope of this study and should be investigated in future work.

When discussing the utilization of excess heat, it is also important to adopt a proper definition of the term. Olsson et al. (2015) define excess heat as "Excess energy that cannot be utilized internally and where the alternative is that the heat is released into the surroundings". Bendig et al. (2013) discuss the important distinction between avoidable and unavoidable excess heat. Pettersson et al. (2020) propose adopting a pragmatic techno-economic perspective whereby avoidable excess heat refers to heat that could be reused internally within the process through heat recovery measures that meet the plant owner's investment performance criteria. The latter definition is adopted in this work and the term "available excess heat" refers to the excess heat that is available for utilization in the CO_2 capture plant under given conditions.

2. Method

Fig. 1 provides an overview of the studied system and the system boundaries considered for different parts of the analysis. To evaluate the potential of different strategies for heat delivery to a CCS unit and a district heating network, two studies were conducted: a generic study that illustrates the effects of the main system characteristics, and a case study that uses real plant data. The generic study determines how the magnitude of excess heat over time affects the suitable choice of design and operation of the capture plant. To estimate the size and performance of the CO_2 capture equipment, a design study was carried out, which included simulations of the capture plant and the compression sequence using Aspen Plus software (v11). Furthermore, an economic assessment was performed, including a sensitivity analysis with respect to key parameters, to compare the economic performance of the heat recovery options. In the case study, the methodology was applied using input data based on historical seasonal variations of excess heat from a steel mill and its integrated off-gas fired CHP plant, and a comparison between prioritizing the district heating network or the CO_2 capture plant as recipient of the excess heat was conducted.

2.1. Setup of the generic study

Five theoretical heat load curves (Fig. 2) were considered in the generic study. The heat displayed in these curves represents the excess heat available at the industrial site for CCS after delivery of heat to the district heating network. Since the district heating demand is low during summer, the peak value is the maximum amount of heat available from the industrial plant. The curves were generated using Eq. (1), in which the two main parameters are the maximum amount of available heat, *MH* (MW), and the length of the season during which excess heat is available for CCS, *SL* (hours).

$$y = MH\cos\left(\frac{\pi}{SL}(x - 4380)\right) \quad (1)$$

The seasonal length of the theoretical heat load curves, shown in Fig. 2, was defined as either short season (Curve 2; excess heat available May-August, 2952 h), medium-long season (Curves 1, 4, and 5; heat available March-October, 5880 h) or long season (Curve 3; heat available all year, 8760 h). The peak of the heat load curves, i.e., the

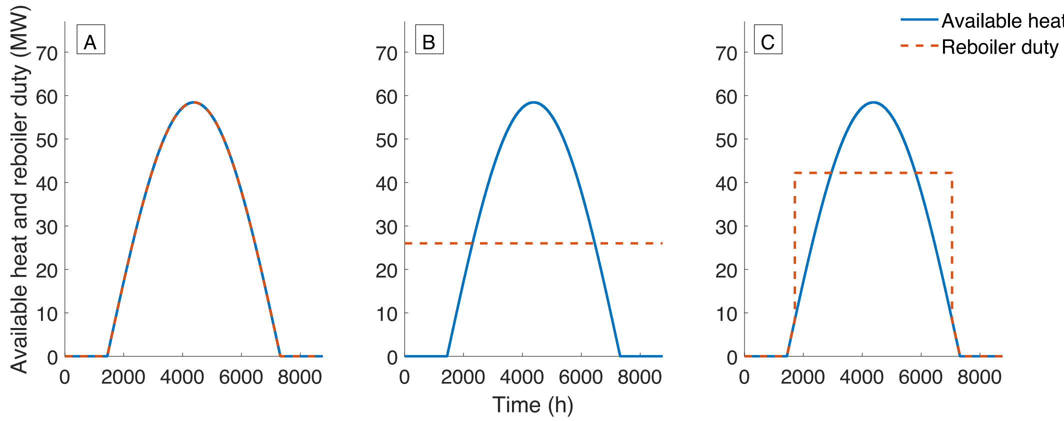

Fig. 3. Illustration of Configurations A, B and C for heat load curve 1.

Table 1
Flue gas specification used in the generic study (adapted from Onarheim et al. (2017)) and the case study (adapted from Biermann et al. (2019)), respectively.

Component/ property	Unit	Generic study	Case study (BFG)
CO_2	mol%	13.0	24.6
H_2O	mol%	17.0	2.2
N_2	mol%	67.7	49.6
O_2	mol%	2.3	0
CO	mol%	0	20.4
H_2	mol%	0	3.2
T	°C	184	29
P	kPa	101.3	181.3
Flow	kNm^3/h	50-497	352.4

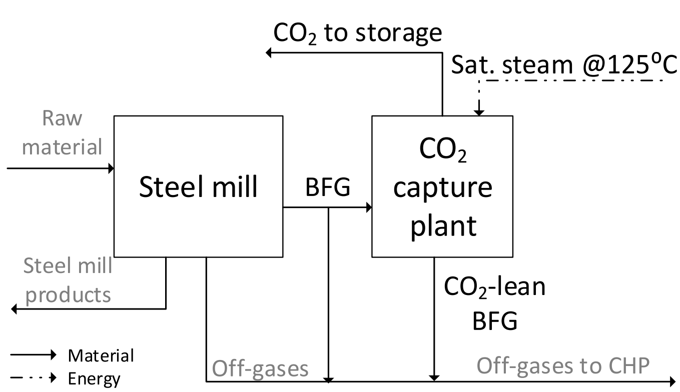

Fig. 4. Overview of the integration between the steel mill, the CO2 capture plant and the CHP plant considered in the case study. The material and energy flows of interest for the study are marked in black, others are grey. BFG = Blast Furnace Gas.

maximum amount of available heat, was defined on the basis of the heat input (MW) to the capture plant reboiler required to achieve a design capture rate of 100, 500 or 1000 kton CO_2/year (12, 58 and 117 MW), corresponding to capture rates of 11, 57 and 114 t CO_2/h respectively.

For each of the 5 excess heat load curves, three CCS plant configurations (i.e. plant size combined with plant operating strategy) were defined as follows and illustrated in Fig. 3:

(1) Configuration A: carbon capture capacity determined by the peak value of available heat, and operated at varying capture rate throughout the year, depending on the availability of excess heat as determined by the heat load curve.
(2) Configuration B: the carbon capture plant operates at constant capture load throughout the year, and is sized to achieve the same annual capture rate as Configuration A.
(3) Configuration C: designed for hybrid operation, i.e. constant capture rate during some parts of the year and reduced capture rate during other parts of the year (following the heat load curve). The capture plant size was set as the average of the plants sizes of Configurations A and B, and the length of the constant capacity operation was adjusted to achieve the same yearly capture rate as in A and B.

Operation for Configurations B and C results in a heat deficit during some parts of the year, which was assumed to be covered by heat generated by combustion of biomass (with assumed CO_2 emissions of 0 g CO_2/MJ_{fuel} and a fuel-to-heat efficiency of 90%). The energy penalty of these configurations was estimated by dividing the primary energy supply (heat supply by combustion of additional fuel) to the total heat input to the capture plant. The degree of utilization of each capture plant was estimated according to Eq. (2). The configurations were compared based on the trade-off between energy penalty and degree of utilization. Assuming a carbon neutral make-up fuel illustrates the best-case scenario, where the carbon dioxide mitigation potential of the capture plant is not affected by its energy demand.

$$Degree\ of\ utilization\ (\%) = \left(\frac{Actual\ capture\ rate\ (kton/a)}{Design\ capture\ rate\ (kton/a)} \times 100\right) \tag{2}$$

The assumed characteristics of the flue gas in the generic study are specified in Table 1. The flue gas composition was determined such that the two following criteria were fulfilled:

(1) CO_2 concentration somewhere in the middle of the normal range of CO_2 content in industrial flue gases, i.e. 5-30 vol%.
(2) Representative values for concentration of other common species such as H_2O and O_2.

The composition, as well as the temperature and pressure, were therefore based on values for the flue gas from a pulp mill recovery boiler, adopted from Onarheim et al. (2017), which fulfills the two criteria described above. The flue gas flow rate was varied to correspond to 100, 500 or 1000 kton/a of captured CO_2 for design point operation, assuming a capture rate of 90%.

2.2. Case study: SSAB integrated steel mill in Luleå

The case study is an integrated steel mill located in Luleå in northern Sweden owned by SSAB with direct plant emissions of about 3.4 $MtCO_2$/a. The most important emitter is the blast furnace, where iron ore is reduced to pig iron using coke or coal, and blast furnace gas (BFG),

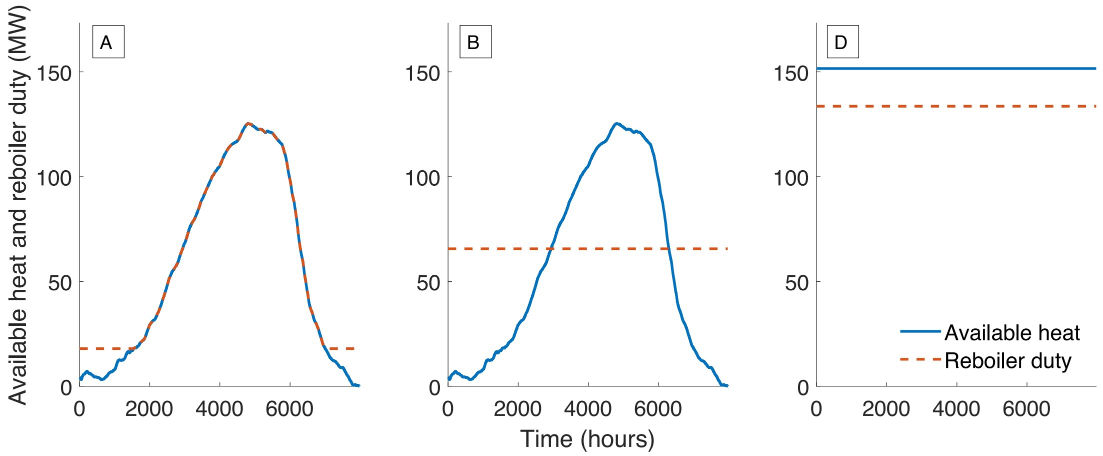

Fig. 5. Available heat and reboiler duty for configurations A, B and D respectively in the case study. Heat load curves were based on the work by Martinez Castilla et al. (2019).

Table 2
Characteristics of the capture plant configurations evaluated in the case study. DH = district heating.

Configuration	A	B	D
Capture plant size criteria	Corresponding to peak amount of available heat	To achieve equal CO_2 avoidance as Conf. A	Corresponding to peak amount of available heat
Design capture rate	144 t/hr	76 t/hr	154 t/hr
Operation	Varying	Constant	Constant
Reboiler duty	Max 125 MW	66 MW	134 MW
DH supply	Unchanged	Unchanged	Decreased
CO_2 avoided	< CO_2 captured	< CO_2 captured	Equal to CO_2 captured

containing considerable amounts of both carbon dioxide and carbon monoxide, is produced as a by-product. In the integrated CHP plant, off-gases (mainly BFG) from the steel mill are combusted to generate process steam, electricity, and district heating.

2.2.1. Studied system

Fig. 4 shows the integration between the steel mill, the CHP plant and the CO_2 capture plant considered in this work. The CO_2 capture plant is located downstream from the steel mill but upstream from the CHP plant. Carbon dioxide is assumed to be captured from the blast furnace gas, since previous studies (see e.g. Biermann et al. (2019)) have pointed out the benefits of capturing carbon dioxide from the blast furnace gas directly instead of applying capture to the flue gas stream after the boiler in the CHP plant, thus, partial capture of the site emissions is applied. The blast furnace gas characteristics are listed in Table 1. Please note that the CO_2 concentration and total pressure are higher than in the generic study; high CO_2 concentration and total pressure both have a positive effect on CO_2 separation energy required. Depending on the availability of heat, either all of the blast furnace gas, or only part of it, is lead through the capture plant, otherwise it is fed directly to the CHP plant together with the rest of the steel mill off-gases. After CO_2 has been captured, the CO_2-lean blast furnace gas is also sent to the CHP to be combusted. In the CHP plant, it is assumed that steam can be extracted at suitable conditions for heat supply to the CCS plant (125°C, saturated).

2.2.2. Definition of heat load curves and configurations

The heat load curve of available heat was determined based on data from Martinez Castilla et al. (2019). All heat delivered to the district heating network was considered as excess heat, and the maximum amount of available heat was calculated from the district heat peak delivery (about 160 MW). In the CHP plant, heat is transferred to the district heating network through two condensers in series, where steam (at 81°C and 95°C, respectively) from the steam turbine is condensed to supply heat to the district heating water. Since the steam utilized for district heating is at lower pressures than the pressure suitable for CCS supply, the amount of available heat was corrected to the pressure required for CCS, resulting in a maximum of about 150 MW of excess heat available for CCS.

Fig. 5 shows the heat load curve and reboiler duty for the configurations evaluated in the case study. The seasonal length was assumed to be equal to the steel mill operating hours (7972 h/a) (Garðarsdóttir et al., 2018). The characteristics of the case study configurations are described hereinafter and summarized in Table 2. Since the district heating demand was around 25 MW during the summer, the peak amount of available heat for Configurations A and B was set to 125 MW (instead of 150 MW available without DH generation). In addition to Configurations A and B, an additional configuration was defined (Configuration D) in which it was assumed that the district heating network only receives excess heat if the CCS demand has been satisfied. Configuration C was not evaluated in the case study. Furthermore, for Configuration A, the capture plant was assumed to operate at a minimum-heat level during periods of little to no available excess heat, since in practice, it may be desirable to avoid shutting down operation of the capture plant (Martinez Castilla et al., 2019). To compensate for the heat deficit in Configurations A and B, combustion of additional natural gas was assumed with an efficiency of 90% (fuel-to-heat) and a CO_2 emission factor of 50 gCO_2/MJ_{fuel} (Song et al., 2004). A fossil fuel was chosen to illustrate the effect of non-carbon neutrality, since it is common that industrial plants use fossil make-up fuels. The capture plant of Configuration B was sized to achieve the same CO_2 avoidance as the capture plant of Configuration A, i.e. the amount of captured CO_2 minus the emissions originating from the additional combustion of fossil fuels. For Configuration D, 134 MW of heat was utilized at a constant load all year, since that amount of heat corresponded to capturing 90% of the CO_2 in the blast furnace gas. Thus, the heat required for maximum capacity of CCS is lower than the maximum amount of available excess heat, enabling a small district heating supply to be maintained for Configuration D as well. However, the effect of the capture plant integration on the CHP outputs were not taken into consideration when evaluating the CO_2 avoided (i.e., CO_2 avoided was equal to CO_2 captured in Configuration D). Although Configuration D imposes a large change in the potential to supply district heating from the steel mill, the loss in district heating supply was not accounted for in the analysis. Furthermore, extracting steam at a higher pressure (see Equation (3)) implies a loss of electric power output from the CHP plant, which can also lead to

Table 3
Simulation specifications, common for all simulations.

Capture plant	Unit	
Absorber packing height	m	20
Stripper packing height	m	15
Lean/rich heat exchanger hot inlet/cold outlet ΔT	°C	10
Stripper overhead pressure	bar(a)	2
Compression sequence		
Discharge pressure compressor 1/2	bar(a)	6.3/20
Intercooling exit temperature	°C	25

Table 4
Simulation specifications applied in the generic study and the case study, respectively. Lean loading and reboiler temperature were optimized to achieve the lowest specific heat input.

Property	Unit	Generic study	Case study
Lean loading	mol CO_2/mol MEA	29	30
Reboiler temperature	°C	121.4	120.9
Lean solvent supply temperature	°C	40	29

Table 5
Assumptions for the economic assessment.

CAPEX		
Cost year	2016	
First- or N:th-of-a-kind	N:th of a kind	
Greenfield or Brownfield	Brownfield	
Location factor	1	
Annualized factor	10.8067	
Plant lifetime	years	25 (including 2 years construction)
Discount rate	%	7.5
Currency conversion[1]	NOK/€	9.7
OPEX		
Fixed OPEX	% of TIC	6
Variable OPEX		
Electricity price[2]	€/MWh	40
Biomass cost[3]	€/MWh_{steam}	20
Natural gas cost[4]	€/MWh_{steam}	18
Cooling water	€/m^3	0.02
MEA	€/m^3	2000
NaOH[3]	€/t	270
Steam[5]	€/t	1

[1] Used in the capture plant CAPEX assessment (2.4.1) since the method by Ali et al. (2019) was developed for NOK.
[2] Average electricity price. The seasonal variations of electricity prices were accounted for as described in 2.4.3.
[3] Used in the economic assessment of the generic study.
[4] Tax-free import price, no distribution cost included. Used in the economic assessment of the case study.
[5] Used in the economic assessment of the case study.

higher emissions depending on alternative grid power plant technology used to compensate for this. If new district heating and/or electricity generation would imply additional carbon emissions, the CO_2 avoided would be smaller than the CO_2 captured also for Configuration D.

2.3. CO_2 capture modeling

The modeling of the CO_2 capture plant, including compression stages up to 20 bar(a) for liquefaction (see boundaries in Fig. 1) was performed using Aspen PLUS v11 simulation software. The capture plant is an absorption-desorption cycle with 30 wt% of MEA as solvent, and the set-up includes rich-solvent splitting (RSS) and absorber intercooling (ICA), based on the work by Garðarsdóttir et al. (2015) and Biermann et al.

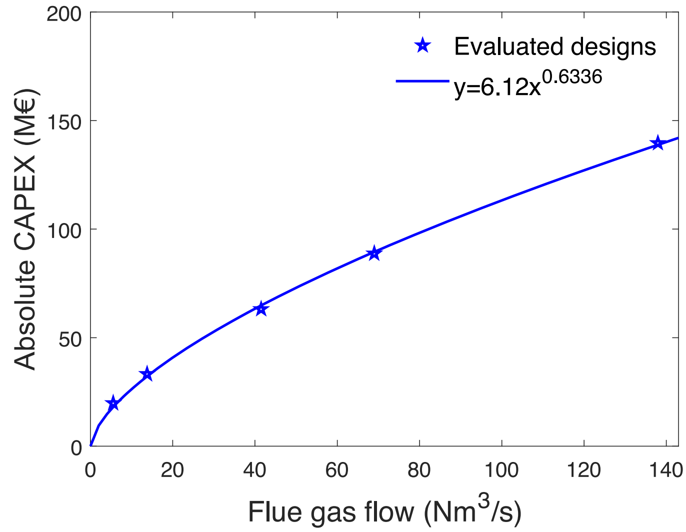

Fig. 6. CAPEX (M€) as a function of flue gas flow (Nm3/s). The CAPEX was evaluated for five designs (indicated by the star symbols), to which a power function was fitted to set up the cost function.

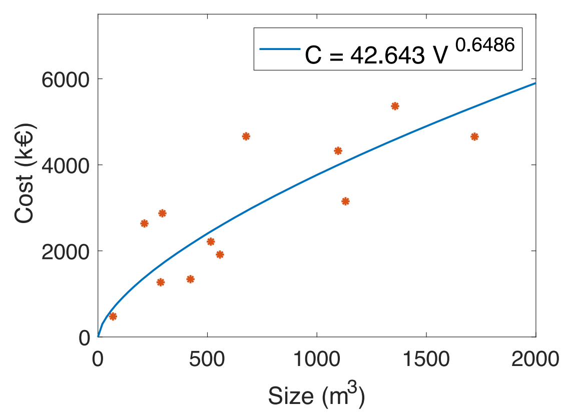

Fig. 7. Cost function for columns, including internals, material: welded SS316. The red dots represent column costs estimated in previous work (Biermann et al., 2019; Gardarsdottir et al., 2019; van der Spek et al., 2017). The blue line shows the power function fitted to the data points. The sizing parameter (V) for columns is the volume in m3.

(2018). The absorber intercooler was only included in the case study, since the addition of ICA has mainly proven important for flue gases with high CO_2 concentrations (Biermann et al., 2018). The direct contact cooler (DCC) was only included in the generic study, since the purpose of the unit is the reduce the water content in the flue gas, as well as to provide cooling prior to the absorber, and the flue gas used in the case study already had low water content and temperature (cf. Table 1).

The CO_2 compression was modeled using the Peng-Robinson with Boston-Mathias extrapolation as vapor property method (Mazzoccoli et al., 2012). The pressure was set to obtain a transport pressure of 7 bar (a) after the liquefaction plant (Deng et al., 2019). Other relevant design specifications of the CO_2 capture and liquefaction plant are listed in Tables 3 and 4, with the latter specifying conditions that generated the lowest specific reboiler duty (i.e. heat input per amount of captured CO_2) for the generic study and the case study respectively. The capture plant was designed for a 90% separation rate in the absorber. This target was achieved by adjusting the lean solvent flow, and the column diameters as well as the main dimensions of other equipment were calculated based on design point simulations. Off-design simulations were also carried out, in which the performance of the capture plant was

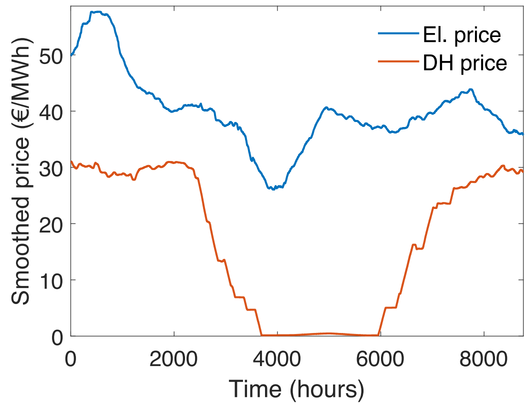

Fig. 8. Seasonally varying electricity prices (blue) and district heating prices (red).

estimated for absorber separation rates of <90%, corresponding to varying heat input to the reboiler.

2.4. Economic assessment

Key assumptions for the economic assessment are listed in Table 5. The CAPEX estimation for the capture plant is described in 2.4.1, and for the compression sequence and liquefaction plant in 2.4.2. In the generic study, the total CAPEX (capture plant, compression sequence and liquefaction plant) was set as a function of the flue gas flow, according to Fig. 6, by estimating the cost of five designs (indicated by star symbols), to which a power function was fitted.

2.4.1. Capture plant

For the capture plant, the cost of the equipment was estimated using sizing parameters. A detailed flow sheet and an equipment list over all included equipment pieces for two evaluated designs can be found in Appendix A. The equipment cost was calculated by equipment-specific cost estimation power functions, which were set up based on cost estimations in previous work (Biermann et al., 2019; Gardarsdottir et al., 2019; van der Spek et al., 2017). For example, the power function used to estimate the cost of columns is displayed in Fig. 7, while the cost functions for other equipment can be found in Appendix B. The equipment installed cost (EIC) was estimated using the enhanced detailed factor (EDF) method as described by Ali et al. (2019). In the EDF method, different factors for direct costs, engineering costs, administration costs, commissioning and contingency are applied based on the absolute value of the equipment cost. The total installed cost (TIC) of the capture plant were obtained by summation of the EIC of individual equipment. The cooling, heating and power duties, as well as the consumption of chemicals (MEA, NaOH) included in the evaluation of operational expenditures (OPEX) were based on the simulations.

2.4.2. Liquefaction plant

For the liquefaction plant, the total direct cost (TDC) was estimated as a single unit by scaling the costs derived by Deng et al. (2019) to the CO_2 flow in this work. The TIC was then obtained by multiplying the TDC with factors for process and project contingency, indirect cost and owner cost in accordance with the method described in Deng et al. (2019). The TIC for the liquefaction plant is equal to the total CAPEX since one single unit is assumed. The compressor duties, and the duties of the intermediate cooling, were obtained from the simulations. The duties for other equipment in the liquefaction plant was estimated based on the work by Deng et al. (2019) by scaling their results to the compression duties and duties of intermediate cooling from the simulations carried out in this work.

2.4.3. Operational expenditures

Assumptions for fixed and variable OPEX, independent of season, are given in Table 5. Seasonally varying electricity prices and district heating prices are given in Fig. 8. The electricity prices are the moving average over 720 h (one week) of spot prices in Sweden (average of SE1-4) in 2019 (NordPool, 2019). The district heating prices are moving averages over 720 h of marginal heat generation cost for the city of Gothenburg, as modelled according to Romanchenko et al. (2020). The seasonally varying electricity price was applied when evaluating the total cost of electricity for the CO_2 capture and liquefaction plant in both the generic study and the case study. The potential loss of revenue due to reduced electric power output from the CHP was however not taken into account as an expense allocated to the capture plant in the case study. The district heating price is important as district heating is the alternative use of the heat used for CCS, and was taken into account in the economic assessment of Configuration D in the case study (cf. Fig. 5), since that configuration imposed a large change to potential to supply district heat. In the generic study, the steam cost was assumed to be zero if only available heat was used, and equal to the fuel cost, (i.e. biomass price divided by fuel-to-heat efficiency), if primary energy was supplied. In the case study, the cost of steam applied when available heat was used was 1 €/t steam, based on the work by Biermann et al. (2019). If primary energy was used, the steam cost was equal to the cost of natural gas (natural gas price divided by fuel-to-heat efficiency).

Table 6
Key performance indicators for Configurations A, B and C (cf. Fig. 3) evaluated in the generic study.

Heat load curve	Heat capacity (MW)	Seasonal length (h)	Configuration	Captured CO_2 (kton/a)	Degree of utilization (%)	Energy penalty (%)
1	58	5880	A/B/C	222	45/100/62	0/43/17
2	58	2952	A/B/C	112	22/100/37	0/67/26
3	58	8760	A/B/C	331	66/100/80	0/22/10
4	117	5880	A/B/C	445	45/100/62	0/43/17
5	12	5880	A/B/C	44	45/100/62	0/43/17

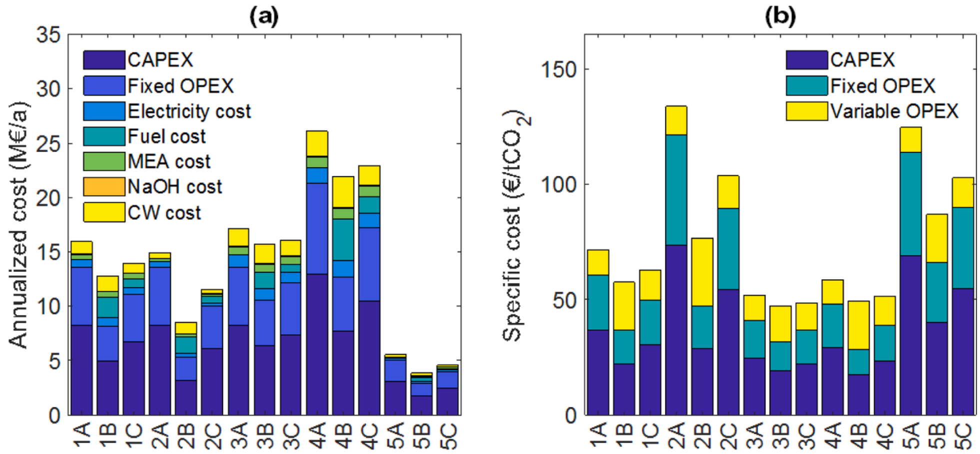

Fig. 9. Economic assessment of the generic study. (a) Annualized cost (CW = cooling water). (b) Specific cost of each configuration.

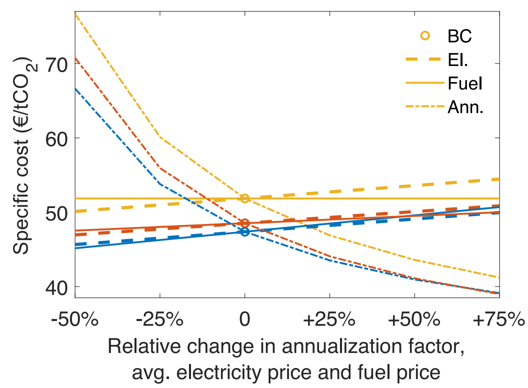

Fig. 10. Sensitivity analysis of the economic assessment of configurations related to curve 3. Investigated parameters are average electricity price (El.), fuel price (Fuel) and annualized factor (Ann.). Configuration A results in yellow, configuration B results in blue and configuration C results in red. The starting point (base case, BC) for each configuration is indicated by the circles.

3. Results

3.1. Generic study

Table 6 shows an overview of key performance indicators for the different configurations depending on the characteristics of the heat availability. Since heat load curves 1, 4 and 5 have the same seasonal length, the degree of utilization and energy penalty is also equal between the corresponding configurations. Comparing curves of different seasonal lengths, it is clear that the seasonal length has an important impact on the degree of utilization obtained for the different configurations, since e.g. a shorter season leads to a smaller capture rate than a longer season. The seasonal length also affects the energy penalty since a longer season implies less need for additional energy supply.

3.1.1. Annualized cost

Fig. 9(a) displays the annualized cost for all evaluated configurations in the generic study. Configuration B has the lowest cost for all investigated heat load curves, which shows that regardless of the excess heat availability, it is more expensive to have a low utilization of the capture plant than of the energy supply system. The effect of the season duration is seen by comparing the results for heat load curves 1- 3. A short season with low district heating demand (heat load curve 2) results in larger differences between the plant sizes, and thus their costs, between configurations, since the degree of utilization of Configurations A and C are lowest for heat load curve 2. Conversely, a long season (heat load curve 3) reduces the differences in utilization between configurations. The effect of economy of scale can be clearly seen by comparing heat load curves 1, 4 and 5, which have the same seasonal length.

3.1.2. Specific cost

Fig. 9(b) shows the specific cost for the configurations evaluated in the generic study. The degree of utilization is clearly reflected in the specific CAPEX: for configuration A, the specific CAPEX is a larger contributor to the total specific cost than for B and C configurations. Note that Fixed OPEX is a factor of the TIC and, thus, responds to the

Table 7
Key performance indicators for the configurations investigated in the case study. The energy penalty for configuration A arises from combustion of natural gas during periods of little or no available excess heat, to avoid having to shut down the capture plant.

Heat load curve	Configuration	Captured CO_2 (kton/a)	Avoided CO_2 (kton/a)	Avoided CO_2 (% of site emissions)	Degree of utilization (%)	Energy penalty (%)
SSAB	A/B	567/603	562	17	49/100	5/39
SSAB	D	1228	1228	36	100	0

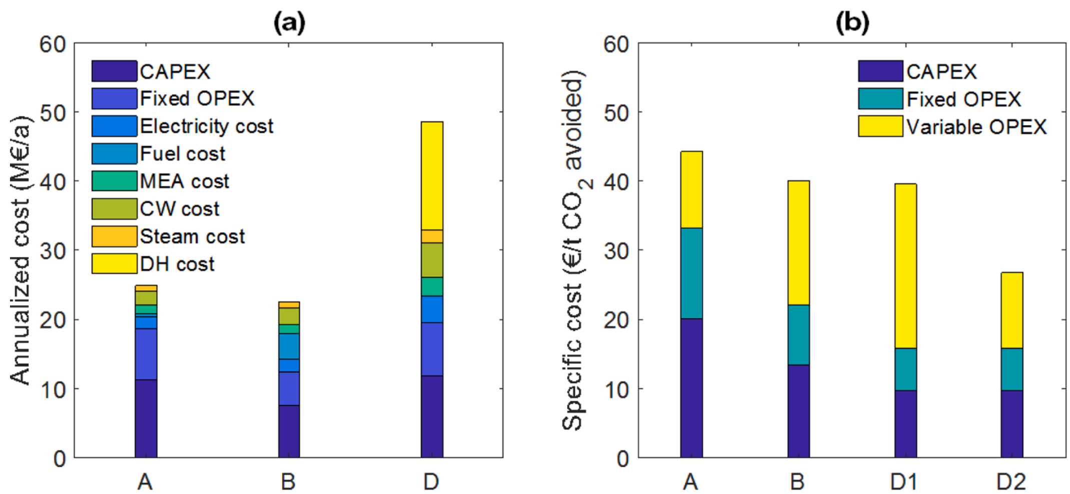

Fig. 11. Economic assessment for the case study configurations. (a) Annualized cost (CW = cooling water, DH = district heating). (b) Specific cost. Configurations A and B have different capture rates but equal CO2 avoidance.

same factors as CAPEX. Short season (heat load curve 2) and small peak of available heat (heat load curve 5) both lead to increased specific costs. In addition, for heat load curves 2 and 5, the specific cost is more sensitive to the choice of configuration compared to other curves. Having either a long season (heat load curve 3) or a high peak of available heat (heat load curve 4) results in similar specific costs, with a long season being slightly less expensive as well as less sensitive to the choice of configuration (i.e. specific costs are more similar among configurations).

3.1.3. Sensitivity analysis

Fig. 10 shows the sensitivity analysis conducted for Configurations A, B and C for heat load curve 3. The sensitivity is shown for heat load curve 3 as the corresponding configurations had a relatively similar performance for this profile. The sensitivity analysis indicates that configuration A is the most expensive for all cases, although favored by reduced CAPEX and increased fuel price. To achieve break-even costs, Configurations B and C require a 50% increase in annualized factor or around a 35% increase in fuel price.

3.2. Case study: SSAB integrated steel mill in Luleå

Table 7 shows the key performance indicators for the configurations investigated in the case study. The performance is similar to the corresponding configurations of heat load curve 4 in the generic study, since both curves have high peak amounts of available heat. Furthermore, even though the seasonal length for the SSAB curve is 7972 h, for a considerable part of the season, the amount of available heat is very low and thus, in reality, the season becomes comparable to the intermediate season length in the generic study. This is reflected by the similarities in degree of utilization of Configuration A, and in energy penalty for Configuration B.

3.2.1. Annualized cost

The annualized costs for the configurations evaluated in the case study are displayed in Fig. 11(a). The annualized costs of Configurations A and B are similar to the ones for heat load curve 4 in the generic study, which is reasonable since both have large peak amounts of available heat. Configurations A and D have almost the same size, which leads to similar values for CAPEX and fixed OPEX. In Configuration D, however, the degree of utilization is higher and thus also the variable OPEX, especially considering that the loss in district heating revenue is accounted for as an expense allocated to the capture plant. For Configuration A, the lower degree of utilization results in CAPEX and fixed OPEX that represents almost 80% of the total annualized cost, while the corresponding share for Configuration B is around 50%.

3.2.2. Specific cost

Fig. 11(b) shows the specific costs for the configurations evaluated in the case study. As in the generic study, Configuration B has a lower specific cost than Configuration A. The specific cost of Configuration D is displayed in two ways; D1 in which the loss of district heating revenue is taken into account, and D2 in which it is not accounted for, with the purpose of clearly illustrating the impact of the district heating revenue on the economic assessment of the capture plant. Configuration D2 shows the lowest specific cost of all configurations. When the loss of district heating revenue is taken into account (D1), the difference between configurations is not as pronounced.

4. Discussion

4.1. Site specific implications

Site specific conditions will have an impact on the cost and feasibility of implementing CO_2 capture. The economic assessment carried out in the generic study (cf. Fig. 9) showed that both scale (i.e. how large the point source of CO_2 is, reflected in the peak of available heat in this work) and season length are important site-specific parameters to consider when evaluating the potential for integration of CCS and district heating. Adopting a seasonally varying operation might be feasible for a large-scale point source with long season, i.e. high availability of heat. This option might be considered if it is desired to retain the district heating supply initially, while having the opportunity to scale-up CCS operation if carbon prices rise. In that sense, implementing a capture plant with low degree of utilization has an advantage, since scale-up of operation of a capture plant with high degree of utilization is not possible without investment in additional CO_2 capture facilities. However, for a smaller point source, or a short season, it is clear that applying a low degree of capture plant utilization is by far the costliest option, thus in that case, such configuration should be avoided. The cost for transport and storage of CO_2 have not been considered in this work. However, these costs would pose a challenge for plants with low capture rate since they are also favored by economy of scale (Roussanaly et al., 2021).

Furthermore, even though a value for the CO_2 intensity of natural gas was considered in the design and economic assessment in the case study, make-up fuels used at industrial plants might have even higher CO_2 intensities (e.g. if oil or coal is used). If higher CO_2 intensities are considered, an increase in both CAPEX and OPEX for a plant with high degree of utilization would be required in order to achieve the same CO_2 avoidance as a capture plant that is operated following the seasonal variations in available heat, which may cause a shift in which the most favorable option is in terms of specific cost. Additionally, to generate steam from combustion of biomass to supply heat to the CO_2 capture plant could require large amounts of scarce resources (Biermann et al., 2019; Karlsson et al., 2021). Hence, it is important to consider the type of energy supply available for CO_2 capture, both with respect to the CO_2 avoidance potential and with respect to the competition of resources, which again supports the conclusion of the advantage of utilizing any available excess heat.

4.2. Utilization

The results from both the generic study and the case study showed that a low plant utilization (Configuration A) is not economically competitive compared to supplying additional primary energy when needed (Configuration B, i.e. low utilization of the available excess heat in the plant energy system), cf. Figs. 9 and 11. Although, the sensitivity analysis (cf. Fig. 10) showed that if the price of fuel for primary energy supply increases significantly (~80-100%), it would become competitive to decrease the utilization of the capture plant. It should be noted, however, that the sensitivity analysis was carried out for the configurations of heat load curve 3, i.e. the curve with the least differences in specific cost among configurations, and the overall highest degree of capture plant utilization. Hence, it is not evident that similar results would be obtained for the other heat load curves, with lower degrees of capture plant utilization.

Furthermore, additional energy supply was considered a utility, i.e. costs associated with additional heat supply capacity were not considered. This assumption implies an excess capacity in the current industrial energy system, which is not necessarily the case. A low utilization of the available excess heat may, thus, result in an increase in the cost of energy not reflected in the present work. Biermann et al. (2021) identified possibilities to utilize both excess heat and excess capacity for CO_2 capture at a refinery and emphasized the importance of considering the potential in the existing plant energy system for cost-efficient implementation of CO_2 capture. Another aspect to consider is that, in the case study, a maximum of 36% of direct plant emissions were captured. Under the assumption that all fossil CO_2 emissions must be eliminated, the energy system at the industrial plant might have to be extended with new infrastructure regardless of the current amount of available excess heat.

4.3. Definition of excess heat

If carbon neutrality is seen as a necessity for industry, the capture plant should reasonably be considered as an internal part of the industrial plant to offset fossil emissions. Hence, since the term excess heat refers to heat that cannot be utilized for internal heat integration, it would be more appropriate to consider that all heat that could be used for CCS is not excess heat. Hence, in contrast to how the term excess heat has been used in other studies related to heat supply to a CCS unit (e.g. Andersson et al. (2016); Biermann et al. (2019)), the term would then refer to heat that cannot be utilized for CCS due to insufficient temperature levels, and/or heat that can be recovered from the capture plant for external heat supply. By adopting such definition, the potential to supply district heating from industrial plants would be highly affected. However, a previous study by the authors has shown that the potential to recover heat from the capture plant for district heating purposes can be significant (~25% of the amount of heat supplied to the CCS unit) (Eliasson et al., 2021). Another consequence of re-defining excess heat is that the energy penalty that was allocated to the capture plant in this study would instead be allocated to the district heating network, which would make constant operation of the capture plant even more favorable compared to the alternatives. However, since there may still be a lack of incentives for implementing CCS, to not be able to supply district heating would cause economic losses for the industrial plant, and potentially increased emissions elsewhere depending on the technology used to replace the heat. When considering the economic impact of lost district heating supply in the case study, implementing CCS with retained district heating supply was seen to have comparable specific capture cost to the configuration where CCS was prioritized (cf. Fig. 11(b)). Thus, it is feasible to apply a capture plant with seasonally varying operation, i.e., low degree of utilization, and retain the district heating supply. The advantage of such an investment is the potential to scale-up operation, since all CO_2 emissions will have to be avoided in order to reach the target of net-zero emissions.

5. Conclusion

In this work, process simulations and an economic assessment of an amine-based CO_2 capture plant were conducted to investigate the interplay between usage of available excess process heat to provide heat for CO_2 capture at the plant site and supplying heat to a district heating network. Different heat load curves, representing seasonal variations of excess heat availability for CO_2 capture, were considered to investigate the relation between utilization of the capture plant and the heat supply system. The results showed that:

(1) The size of the CO_2 point source and the length of the period during which excess heat is available are important parameters for achieving cost-efficient co-integration of industrial carbon capture and district heating supply.
(2) A low degree of utilization of the capture plant has a more pronounced impact on the total annual cost than a low degree of utilization of the available excess heat. A significant increase in fuel prices (at least by 100%) is needed for seasonally varying operation of the capture plant to become economically competitive compared to the alternative of supplying primary energy, even when capture plant utilization is relatively high.
(3) Accounting for the loss of revenue from district heating supply when evaluating the cost of capture plant integration has a significant impact on the specific capture cost and can make seasonally varying operation comparable in cost to the alternative where CCS is prioritized for usage of excess heat (44 €/t CO_2 avoided for the former, 40 €/t CO_2 avoided for the latter). If maintaining the amount of district heating supplied is not prioritized, specific capture costs of 29 €/t CO_2 avoided can be achieved.

Declaration of Competing Interest

The authors declare that they have no known competing financial interests or personal relationships that could have appeared to influence the work reported in this paper

Acknowledgement

This work was conducted within the framework of the Preem CCS project with funding provided by Preem AB, SINTEF Energi AS, Aker Carbon Capture, Equinor, the Norwegian CLIMIT Programme and the Swedish Energy Agency.

Appendix A

Fig. 12 shows a detailed flow sheet of the CO_2 capture plant, including all equipment pieces for whom which individual costs were

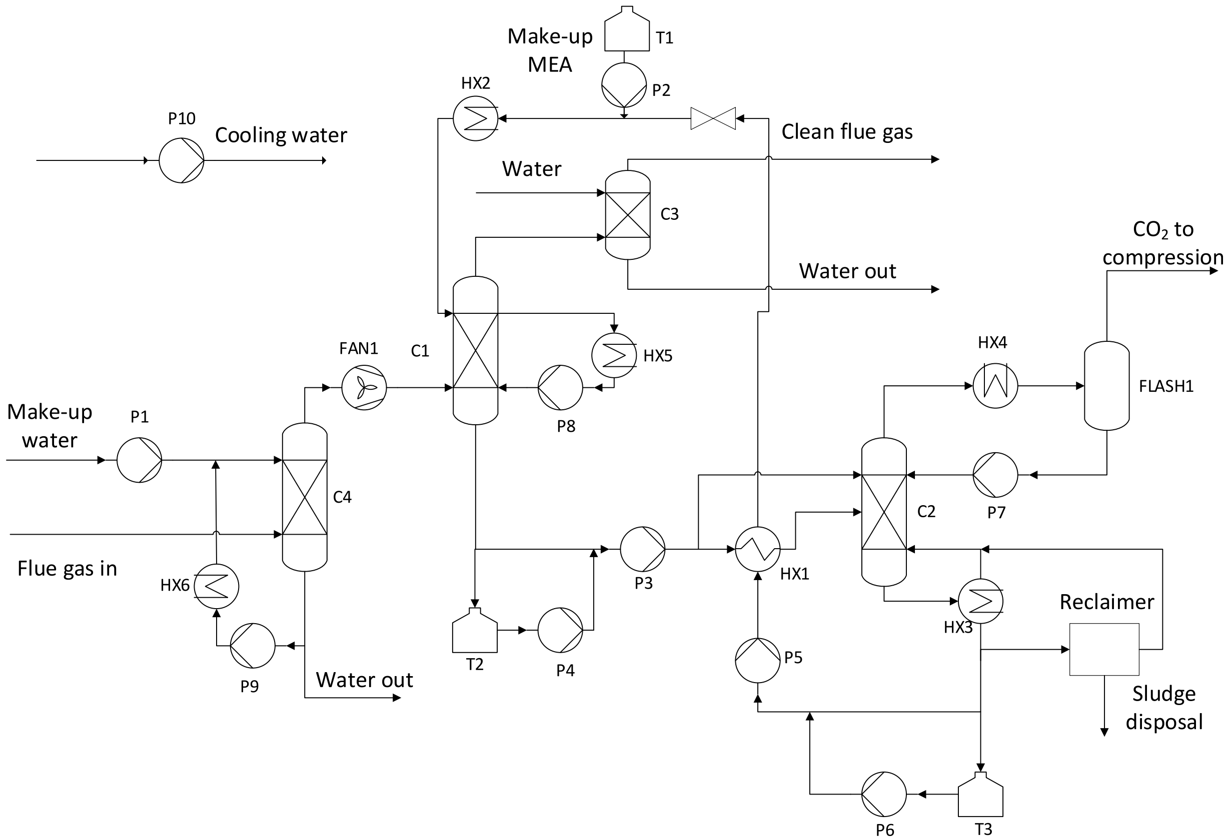

Fig. 12. Detailed flow sheet of the CO2 capture plant in this study.

Table 8
Equipment list describing the different pieces of equipment included in this work. Included designs are the one of Configuration A of heat load curve 4 in the generic study, and Configuration D in the case study. d = diameter, h = total height, KO = knock-out.

Equipment	ID	Type	Case study		Generic study	
			Size	EIC	Size	EIC
Columns			m^3	k€	m^3	k€
Absorber	C1	Packed column	1382 (d 7.9, h 28.5)	12218	2343 (d 10.2, h 28.5)	17202
Stripper	C2	Packed column	724 (d 6.6, h 21.4)	8032	630 (d 6.12, h 21.4)	7335
Washer	C3	Packed column	82 (d 7.9, h 1.7)	2601	378 (d 10.2, h 4.6)	6357
Direct contact cooler	C4	Packed column	-	-	765 (d 9.4, h 16.2)	8325
Heat exchangers			m^2		m^2	
Lean/ rich heat exchanger	HX1	Shell and tube	15107	9969	9799	8094
Lean solvent cooler	HX2	Shell and tube	2640	2680	2011	2089
Stripper reboiler	HX3	Reboiler	48444	32729	47035	31912
Stripper condenser	HX4	Shell and tube	1624	1718	1703	1794
Absorber intercooler	HX5	Shell and tube	4500	3973	-	-
DCC reflux cooler	HX6	Shell and tube	-	-	5886	5078
Pumps			kW		kW	
Water make-up	P1	Centrifugal	0.007	13	6	218
MEA make-up	P2	Centrifugal	0.001	3	0.03	30
Rich pump	P3	Centrifugal	48	619	71	781
Rich make-up	P4	Centrifugal	24	409	20	456
Lean pump	P5	Centrifugal	306	1301	251	1155
Lean make-up	P6	Centrifugal	31	470	25	417
Stripper reflux pump	P7	Centrifugal	3	146	3.4	158
Absorber intercooler pump	P8	Centrifugal	99.6	814	-	-
DCC reflux pump	P9	Centrifugal	-	-	97.1	802
Cooling water pump	P10	Centrifugal	976	2613	910	2507
Tanks			m^3			
MEA make-up	T1		10	292	60	743
Rich solvent make-up	T2		10	292	10	292
Lean solvent make-up	T3		10	292	10	292
Other						
Reclaimer			29 kg HSS/hr	2884	24 kg HSS/hr	2524
Condenser KO drum	FLASH1		65 m^3 (d 3.6, h 6.4)	784	46 m^3 (d 3.1, h 6.0)	621
Flue gas fan[1]	FAN1		349 kW	954	774	1353
Pre and post filter	-		-	76	-	76
Active carbon filter	-		-	217	-	217
MEA first fill[1]	-		532 m^3	1063	446 m^3	892

[1] Material: Carbon steel

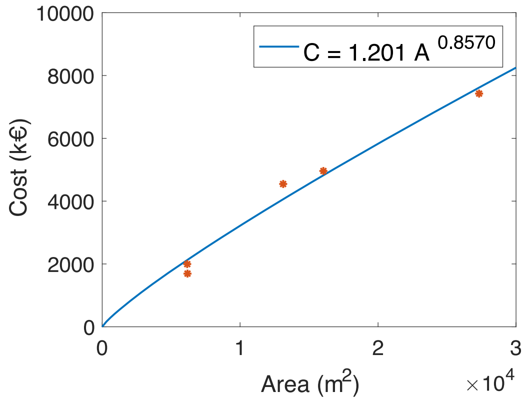

Fig. 13. Reboiler cost function, material: welded SS316. The sizing parameter (A) for the reboiler is the total heat exchanger area (m2).

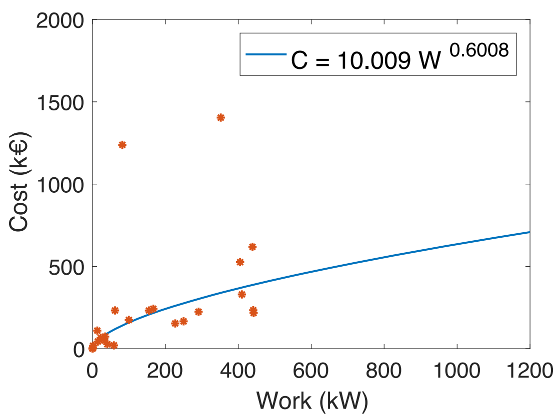

Fig. 14. Pump cost function, material: machined SS316. The sizing parameter (W) for pumps is the required work (kW).

estimated according to 2.4.1. Table 8 shows equipment lists for the capture plant of Configuration A of heat load curve 4 in the generic study, and the capture plant of Configuration D in the case study. Packing in columns is Sulzer Mellapak 250Y, and total height of columns is 1.425 times the packing height. The material is stainless steel for all equipment unless other is specified. Table 8 also includes the cost of MEA first-fill in the capture plant, which was estimated under the assumption of a MEA residence time of 40 min (Montañés et al., 2018).

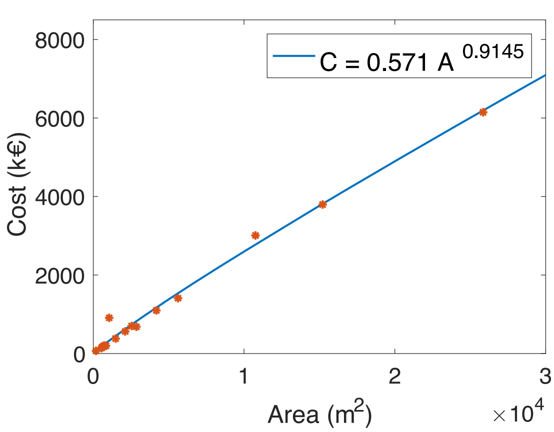

Fig. 15. Cost function for heat exchangers (other than reboiler), material: welded SS316. The sizing parameter (A) for the heat exchangers is the total heat exchanger area (m2).

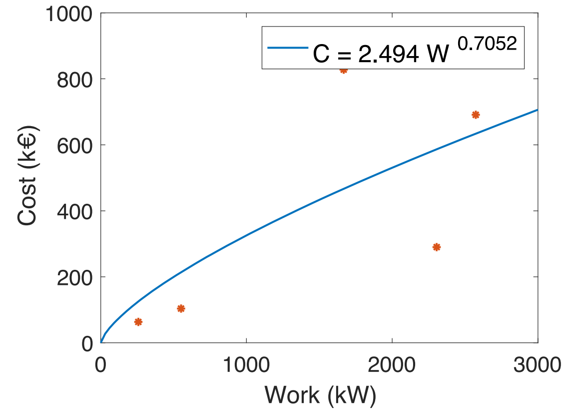

Fig. 16. Flue gas fan cost function, material: carbon steel. The sizing parameter (W) for the flue gas fan is the required work (kW).

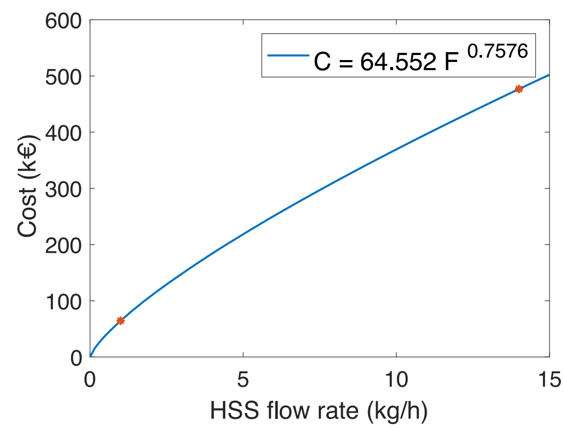

Fig. 17. Cost function reclaimer, material: welded SS316. The sizing parameter (F) for the reclaimer is the HSS flow rate (kg/h).

Appendix B

Figs. 7 and 13–17 shows the cost functions used for estimating the cost of the different equipment pieces in the capture plant, with equipment cost displayed on the y-axis and the sizing parameter displayed on the x-axis. The data points (red dots in the figures) from which the power functions are fitted to were gathered from equipment cost data from Biermann et al. (2019); Gardarsdottir et al. (2019); van der Spek et al. (2017), which were converted to a common cost year (2015) using the chemical engineering plant cost index (CEPCI). To estimate the TIC, the equipment costs of all individual equipment were estimated from the power functions using the sizing parameters as input. The equipment costs then needed to be converted to the desired cost year (2016 in this work). The EIC's were obtained by multiplying the equipment costs with individual factors in accordance with the EDF method as described by Ali et al. (2019), whereby the TIC was obtained by summation of the EIC's. Note that these cost functions give an order-of-magnitude estimate and are inferior to detailed case-by-case assessments using e.g. Aspen Process Economic Analyzer, however they serve the purpose of such high-level studies as this one.

References

Ali, H., Eldrup, N.H., Normann, F., Skagestad, R., Øi, L.E., 2019. Cost estimation of CO_2 absorption plants for CO_2 mitigation – method and assumptions. Int. J. Greenh. Gas Control 88, 10–23. https://doi.org/10.1016/j.ijggc.2019.05.028.

Andersson, J., 2020. An Investigation of Carbon Capture Technologies for Sävenäs Waste-To-Energy Plant. Department of Civil, Environmental and Natural Resources Engineering, Luleå University of Technology, Luleå, Sweden. MSc thesis report.

Andersson, V., Franck, P.Å., Berntsson, T., 2016. Techno-economic analysis of excess heat driven post-combustion CCS at an oil refinery. Int. J. Greenh. Gas Control 45, 130–138. https://doi.org/10.1016/j.ijggc.2015.12.019.

Bartela, L., Skorek-Osikowska, A., Kotowicz, J., 2014. Economic analysis of a supercritical coal-fired CHP plant integrated with an absorption carbon capture installation. Energy 64, 513–523. https://doi.org/10.1016/j.energy.2013.11.048.

Bendig, M., Maréchal, F., Favrat, D., 2013. Defining "Waste Heat" for industrial processes. Appl. Therm. Eng. 61 (1), 134–142. https://doi.org/10.1016/j.applthermaleng.2013.03.020.

Biermann, M., Ali, H., Sundqvist, M., Larsson, M., Normann, F., Johnsson, F., 2019. Excess heat-driven carbon capture at an integrated steel mill-considerations for capture cost optimization. Int. *J. Greenh. Gas Control* 91, 102833. https://doi.org/10.1016/j.ijggc.2019.102833.

Biermann, M., Langner, C., Eliasson, Å., Normann, F., Harvey, S., Johnsson, F., 2021. Partial capture from refineries through utilization of existing site energy systems. In: Proceedings of the 15th Greenhouse Gas Control Technologies Conference. https://doi.org/10.2139/ssrn.3820101.

Biermann, M., Normann, F., Johnsson, F., Skagestad, R., 2018. Partial carbon capture by absorption cycle for reduced specific capture cost. Ind. Eng. Chem. Res. 57 (45), 15411–15422. https://doi.org/10.1021/acs.iecr.8b02074.

Broberg Viklund, S., Johansson, M.T., 2014. Technologies for utilization of industrial excess heat: Potentials for energy recovery and CO2 emission reduction. Energy Convers. Manag. 77, 369–379. https://doi.org/10.1016/j.enconman.2013.09.052.

Connolly, D., Lund, H., Mathiesen, B.V., Werner, S., Möller, B., Persson, U., Boermans, T., Trier, D., Østergaard, P.A., Nielsen, S., 2014. Heat Roadmap Europe: Combining district heating with heat savings to decarbonise the EU energy system. Energy Policy 65, 475–489. https://doi.org/10.1016/j.enpol.2013.10.035.

Deng, H., Roussanaly, S., Skaugen, G., 2019. Techno-economic analyses of CO_2 liquefaction: Impact of product pressure and impurities. Int. J. Refrig. 103, 301–315. https://doi.org/10.1016/j.ijrefrig.2019.04.011.

Eliasson, Å., Fahrman, E., Biermann, M., Normann, F., Harvey, S., 2021. Integration of industrial CO_2 capture with district heating networks: a refinery case study. In: Proceedings of the TCCS-11 - Trondheim Conference on CO_2 Capture, Transport and Storage, pp. 197–201. Trondheim, Norway - June 22-232021.

Eriksson, L., Morandin, M., Harvey, S., 2018. A feasibility study of improved heat recovery and excess heat export at a Swedish chemical complex site. Int. J. Energy Res. 42 (4), 1580–1593. https://doi.org/10.1002/er.3950.

Feron, P.H.M., Cousins, A., Jiang, K., Zhai, R., Garcia, M., 2020. An update of the benchmark post-combustion CO_2-capture technology. Fuel 273, 117776. https://doi.org/10.1016/j.fuel.2020.117776.

Gardarsdottir, S.O., De Lena, E., Romano, M., Roussanaly, S., Voldsund, M., Pérez-Calvo, J.F., Berstad, D., Fu, C., Anantharaman, R., Sutter, D., Gazzani, M., Mazzotti, M., Cinti, G., 2019. Comparison of technologies for CO_2 capture from cement production-part 2: cost analysis. Energies 12 (3), 542. https://www.mdpi.com/1996-1073/12/3/542.

Gardarsdóttir, S.Ó., Normann, F., Andersson, K., Johnsson, F., 2015. Postcombustion CO_2 capture using monoethanolamine and ammonia solvents: the influence of CO_2 concentration on technical performance. Ind. Eng. Chem. Res. 54 (2), 681–690. https://doi.org/10.1021/ie503852m.

Garðarsdóttir, S.Ó., Normann, F., Skagestad, R., Johnsson, F., 2018. Investment costs and CO_2 reduction potential of carbon capture from industrial plants-a Swedish case study. Int. J. Greenh. Gas Control 76, 111–124. https://doi.org/10.1016/j.ijggc.2018.06.022.

Hammar, C., 2022. Heat integration between CO2 Capture and Liquefaction and a CHP Plant: Impact on Electricity and District Heating Delivery at Renova's CHP Plant in Sävenäs. Division of Energy Technology, Chalmers University of Technology, Göteborg, Sweden. MSc thesis project report.

Huang, Z., Li, J., Jing, C., An, H., Tong, Y., Xie, B., Zhao, Y., Li, C., 2017. Thermal integration of postcombustion CO_2 capture in existing natural gas combined cycle combined heat and power plant. J. Energy Eng. 143 (5), 04017025 https://doi.org/10.1061/(ASCE)EY.1943-7897.0000455.

IEA. (2020). *CCUS in clean energy transitions*. https://www.iea.org/reports/ccus-in-clean-energy-transitions.

Ivner, J., Broberg Viklund, S., 2015. Effect of the use of industrial excess heat in district heating on greenhouse gas emissions: a systems perspective. Resour. Conserv. Recycl. 100, 81–87. https://doi.org/10.1016/j.resconrec.2015.04.010.

Johnsson, F., Normann, F., Svensson, E., 2020. Marginal abatement cost curve of industrial CO_2 capture and storage – a Swedish case study. Front. Energy Res. 8, 175. https://doi.org/10.3389/fenrg.2020.00175.

Jönsson, J., Algehed, J., 2010. Pathways to a sustainable European kraft pulp industry: Trade-offs between economy and CO_2 emissions for different technologies and system solutions. Appl. Therm. Eng. 30 (16), 2315–2325. https://doi.org/10.1016/j.applthermaleng.2010.01.025.

Karlsson, S., Eriksson, A., Normann, F., Johnsson, F., 2021. CCS in the pulp and paper industry – implications on regional biomass supply. In: Proceedings of the 15th Greenhouse Gas Control Technologies Conference. https://doi.org/10.2139/ssrn.3820355.

Manz, P., Kermeli, K, Persson, U., Neuwirth, M., Fleiter, T., Crijns-Graus, W., 2021. Decarbonizing district heating in EU-27 + UK: how much excess heat is available from industrial sites? Sustainability 13 (3), 1439. https://doi.org/10.3390/su13031439.

Martinez Castilla, G., Biermann, M., Montañés, R.M., Normann, F., Johnsson, F., 2019. Integrating carbon capture into an industrial combined-heat-and-power plant: performance with hourly and seasonal load changes. Int. J. Greenh. Gas Control 82, 192–203. https://doi.org/10.1016/j.ijggc.2019.01.015.

Mazzoccoli, M., Bosio, B., Arato, E., 2012. Analysis and comparison of equations-of-state with p-?-T experimental data for CO_2 and CO_2-mixture pipeline transport. Energy Procedia 23, 274–283. https://doi.org/10.1016/j.egypro.2012.06.052.

Montañés, R.M., Flø, N.E., Nord, L.O., 2018. Experimental results of transient testing at the amine plant at technology centre mongstad: open-loop responses and performance of decentralized control structures for load changes. Int. J. Greenh. Gas Control 73, 42–59. https://doi.org/10.1016/j.ijggc.2018.04.001.

Möller, B., Wiechers, E., Persson, U., Grundahl, L., Søgaard Lund, R., Mathiesen, B.V., 2019. Heat roadmap europe: towards EU-Wide, local heat supply strategies. Energy 177, 554–564. https://doi.org/10.1016/j.energy.2019.04.098.

NordPool. (2019). *Historical market data: elspot prices 2019 hourly EUR*. https://www.nordpoolgroup.com/historical-market-data/.

Oh, S.Y., Binns, M., Cho, H., Kim, J.K., 2016. Energy minimization of MEA-based CO_2 capture process. Appl. Energy 169, 353–362. https://doi.org/10.1016/j.apenergy.2016.02.046.

Olsson, L., Wetterlund, E., Söderström, M., 2015. Assessing the climate impact of district heating systems with combined heat and power production and industrial excess heat. Resour. Conserv. Recycl. 96, 31–39. https://doi.org/10.1016/j.resconrec.2015.01.006.

Onarheim, K., Santos, S., Kangas, P., Hankalin, V., 2017. Performance and costs of CCS in the pulp and paper industry part 1: performance of amine-based post-combustion CO_2 capture. Int. J. Greenh. Gas Control 59, 58–73. https://doi.org/10.1016/j.ijggc.2017.02.008.

Pelda, J., Stelter, F., Holler, S., 2020. Potential of integrating industrial waste heat and solar thermal energy into district heating networks in Germany. Energy 203, 117812. https://doi.org/10.1016/j.energy.2020.117812.

Pettersson, K., Axelsson, E., Eriksson, L., Svensson, E., Berntsson, T., Harvey, S., 2020. Holistic methodological framework for assessing the benefits of delivering industrial excess heat to a district heating network. Int. J. Energy Res. 44 (4), 2634–2651. https://doi.org/10.1002/er.5005.

Rogelj, J., D. Shindell, K. Jiang, S. Fifita, P. Foster, V. Ginzburg, C. Handa, H. Kheshgi, S. Kobayashi, E. Kriegler, L. Mundaca, R. Séférian, M. V. Vilariño. (2018). Mitigation Pathways Compatible with 1.5°C in the Context of Sustainable Development. In Global Warming of 1.5°C. An IPCC Special Report on the impacts of global warming of 1.5°C above pre-industrial levels and related global greenhouse gas emission pathways, in the context of strengthening the global response to the threat of climate change, sustainable development, and efforts to eradicate poverty. [Masson-Delmotte, VP. Zhai, H.O. Pörtner, D. Roberts, J. Skea, P.R. Shukla, A. Pirani, W. Moufouma-Okia, C. Péan, R. Pidcock, S. Connors, J.B.R. Matthews, Y. Chen, X. Zhou, M.I. Gomis, E. Lonnoy, T. Maycock, M. Tignor, T. Waterfield (eds.)].

Romanchenko, D., Nyholm, E., Odenberger, M., Johnsson, F., 2020. Balancing investments in building energy conservation measures with investments in district heating-a Swedish case study. Energy Build. 226, 110353 https://doi.org/10.1016/j.enbuild.2020.110353.

Roussanaly, S., Berghout, N., Fout, T., Garcia, M., Gardarsdottir, S., Nazir, S.M., Ramirez, A., Rubin, E.S., 2021. Towards improved cost evaluation of carbon capture and storage from industry. Int. J. Greenh. Gas Control 106, 103263. https://doi.org/10.1016/j.ijggc.2021.103263.

Song, C., Pan, W., Srimat, S.T., Zheng, J., Li, Y., Wang, Y.H., Xu, B.Q., Zhu, Q.M., 2004. Tri-reforming of methane over Ni catalysts for CO_2 conversion to syngas with desired H_2/CO ratios using flue gas of power plants without CO_2 separation. In: Park, S.E., Chang, J.S., Lee, K.W. (Eds.), Tri-reforming of methane over Ni catalysts for CO_2 conversion to syngas with desired H_2/CO ratios using flue gas of power plants without CO_2 separation. Stud. Surf. Sci. Catal 153, 315–322. https://doi.org/10.1016/S0167-2991(04)80270-2.

Sundqvist, M., Biermann, M., Normann, F., Larsson, M., Nilsson, L., 2018. Evaluation of low and high level integration options for carbon capture at an integrated iron and steel mill. Int. J. Greenh. Gas Control 77, 27–36. https://doi.org/10.1016/j.ijggc.2018.07.008.

van der Spek, M., Sanchez Fernandez, E., Eldrup, N.H., Skagestad, R., Ramirez, A., Faaij, A., 2017. Unravelling uncertainty and variability in early stage techno-economic assessments of carbon capture technologies. Int. J. Greenh. Gas Control 56, 221–236. https://doi.org/10.1016/j.ijggc.2016.11.021.

Werner, S., 2017. District heating and cooling in Sweden. Energy 126, 419–429. https://doi.org/10.1016/j.energy.2017.03.052.